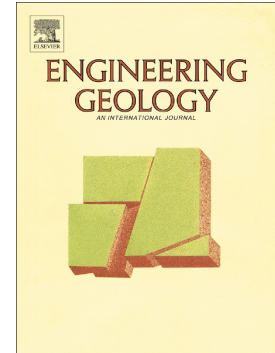# Journal Pre-proof

Redundancy and coherence of multi-method displacement monitoring data as key issues for the analysis of extremely slow landslides (Isarco valley, Eastern Alps, Italy)

Lucia Simeoni, Francesco Ronchetti, Alessandro Corsini

Please cite this article as: L. Simeoni, F. Ronchetti and A. Corsini, Redundancy and coherence of multi-method displacement monitoring data as key issues for the analysis of extremely slow landslides (Isarco valley, Eastern Alps, Italy), *Engineering Geology* (2020), https://doi.org/10.1016/j.enggeo.2020.105504

This is a PDF file of an article that has undergone enhancements after acceptance, such as the addition of a cover page and metadata, and formatting for readability, but it is not yet the definitive version of record. This version will undergo additional copyediting, typesetting and review before it is published in its final form, but we are providing this version to give early visibility of the article. Please note that, during the production process, errors may be discovered which could affect the content, and all legal disclaimers that apply to the journal pertain.

Redundancy and coherence of multi-method displacement monitoring data as key issues for the analysis of extremely slow landslides (Isarco valley, Eastern Alps, Italy)

Lucia Simeoni [a*], Francesco Ronchetti [b], Alessandro Corsini [b]

[a] Department of Civil, Environmental and Mechanical Engineering, University of Trento, via Mesiano 77, 38123 Trento, Italy.

[b] Department of Chemical and Geological Sciences, University of Modena and Reggio Emilia, Via Campi 103, Modena, Italy

e-mail address: francesco.ronchetti@unimore.it, alessandro.corsini@unimore.it

* Corresponding Author: Università degli Studi di Trento, Dipartimento di Ingegneria Civile, Ambientale e Meccanica (DICAM), via Mesiano 77, 38123 Trento, Italy. Tel. +39 0461 282520. e-mail address: lucia.simeoni@unitn.it

Abstract

The paper describes the study of two extremely slow, active-continuous, deep-seated landslides located in the Isarco Valley (Eastern Alps, Italy): a Multiple Rotational Rock Slide (MRRS) and partial reactivation of a Deep-Seated Gravitational Slope Deformation (DSGSD). Both landslides interact with viaducts on the E45 highway. Extensive multi-method field investigation, monitoring of surface and subsurface displacements and limit equilibrium stability analyses were adopted to fully characterize slope dynamics. In order to overcome the limitations due to the systematic errors affecting each single monitoring system and analysis method, an operative framework based on redundancy and coherence tests was introduced to check the reliability of the data and results. In this framework, the geological and geotechnical models of the investigated slopes were progressively refined. This allowed assessment of the type of interaction between the slopes and the highway viaducts.

Highlights

- Study of large, composite and extremely slow landslides requires extensive multi-method monitoring of displacements

- Systematic errors affecting the measurements may mask the actual rate of movement

- Redundancy and coherence tests of monitoring data as a tool to check reliability of data and results

- The reliability of displacement monitoring is crucial to analyse large extremely slow landslides

Keywords:

Extremely slow deep-seated landslides, Field monitoring, Data reliability, Interaction with infrastructures, Eastern Alps

1. Introduction

Extremely slow landslides exhibit displacement rates of less than 16 mm/year (Cruden & Varnes, 1996), in either seasonal or continuous mode (active-intermittent or active-continuous, according to Flageollet, 1996). Extremely slow landslides may be imperceptible without instruments, but in the long term can cause significant damage to the built environment (Mansour et al., 2011) or transport infrastructures (Bidwell et al., 2010; Macciotta et al., 2015). Given the great extent of critical infrastructure that could suffer significant damage in the long term, slow moving landslides are likely to have greater socio-economic impact in more highly developed countries. Mass movements with these characteristics include multiple retrogressive rotational slides (Eisbacher and Clague, 1984), as well as deep-seated gravitational slope deformations (Crosta et al., 2013), i.e. a gravity-induced process affecting large portions of slope evolving over very long periods of time, involving hundreds of millions of cubic meters with thicknesses of up to a few hundred meters (Soldati 2013). The long-term displacement trends of extremely slow landslides may be classified as linear (stationary), convex (periodic acceleration followed by progressive deceleration) or concave (progressive acceleration) (Cascini et al., 2014). In most cases, extremely slow landslides exhibit stationary or convex displacement trends (Glastonbury and Fell, 2008). However, under specific site conditions, landslides exhibiting concave displacement trends may undergo a progressive transition to catastrophic rock avalanches (Crosta et al., 2004; Carey et al., 2007).

Assessment of displacement trends and slope-scale dynamics in large extremely slow landslides is generally challenging, since it requires extensive long-term multi-method monitoring in order to detect complex displacement patterns over wide areas and, ultimately, to cross-check data consistency. Integration of topographic-geodetic methods with geotechnical-geophysical techniques is a possible solution for assessing very slow-moving landslides at specific slope locations (Macfarlane, 2009; Di Maio et al., 2010; Puzrin and Schmid, 2012; Longoni et al., 2017; Palis et al., 2017). Conversely, for their wide-area detection capability, space-borne and ground-based InSAR can make a significant contribution to assessing differential dynamics at slope scale (Strozzi et al.,

2005; Corsini et al., 2006; Noferini et al., 2007; Cascini et al., 2010; Cohen-Waeber et al., 2013; Corominas et al., 2014; Wasowski and Bovenga, 2014, Raspini et al. 2018). The precautionary monitoring of extremely slow landslides nevertheless still requires integration of space-borne techniques with ground-based geotechnical techniques, better suited for detecting very small displacement rates and not affected by motion direction (Wasowski and Pisano, 2019). The redundancy of data from the different monitoring methods is essential in order to overcome the limitations due to the systematic errors affecting each single monitoring system, possibly masking the actual rate of movement (Simeoni and Ferro, 2015). At the same time, coherence between the results from different techniques can corroborate the assessments employed to transform the monitoring data into relevant information to define the geological and geotechnical models at slope scale. Within such a framework, this paper deals with two case studies of large, composite and extremely slow landslides located in the Isarco Valley (Eastern Alps, Italy, Fig. 1) with the aim of: assessing the characteristics and dynamics of the analysed landslides and verifying the extent to which they interact with the affected highway viaducts; highlighting how redundancy and coherence between the results obtained from different monitoring methods can be key issues for improving assessment of complex geological and geotechnical models at slope scale and supporting back-analysis of slope stability conditions.

The Isarco Valley is a glacial valley carved in volcanic rocks (to the south) and metamorphic rocks (to the north). According to Crosta et al. (2013), the valley was affected by a maximum ice thickness of up to 1800 m during the Last Glacial Maximum. Glacial and late-glacial deposits, together with post-glacial and Holocene alluvial terraces, alluvial cones and landslides, are consequently the most widespread deposits and landforms in an Alpine environment that is at present characterized by mean precipitation of around 1000 mm/year and a mean annual temperature of 10°C. The Isarco River Valley is part of the Scandinavian-Mediterranean corridor of the Trans-European Transport Network (TEN-T), which in this section connects northern Italy to Austria by means of the Verona-Brenner railway line. Along the same valley, the transport network

is completed by the SS12 State Road and, most importantly, the E45 highway, which passes mostly through tunnels and over viaducts, partly to reduce exposure to rock falls (Fenti et al., 1977).

The two deep-seated landslides dealt with in this paper interact with viaducts at km 58 and km 70 of the E45 highway and the landslides are therefore referred to as V58 (Fig.1c) and V70 (Fig.1b). Specifically, the E45 viaducts interacting with V58 and V70, built in the mid-1970s, have shallow foundations and show deformation of the elastomeric pads due to relative pier-deck displacements and slight leaning of some piers. Such damage was first recognized in the early 1990s at V70 and around the year 2000 at V58, leading to the investigation and monitoring campaigns on which this paper is based and to substitution of the most deformed elastomeric pads.
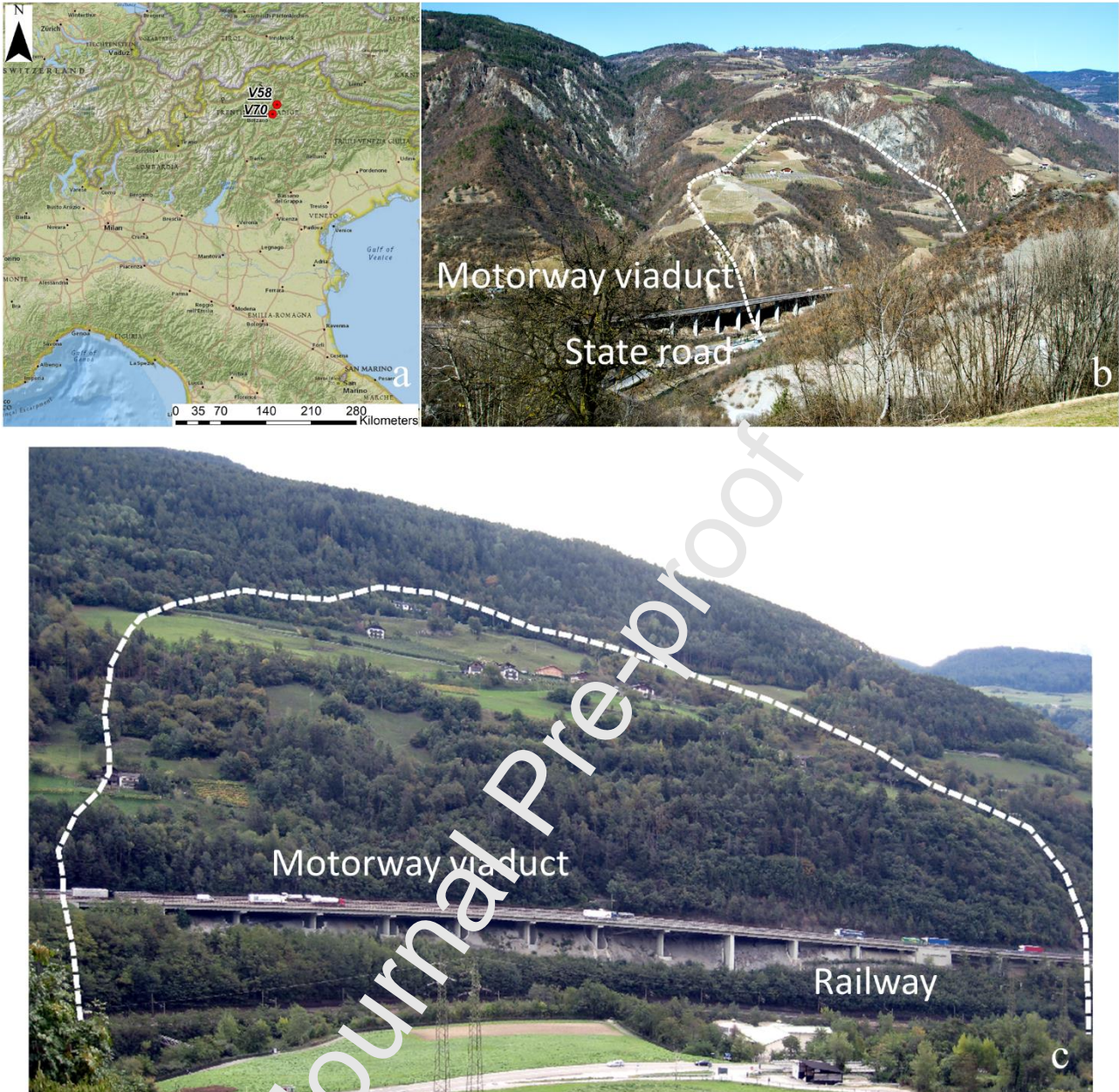
Fig. 1 – (a) Location of the two landslides in Northern Italy. (b) Landslide V70 (deep-seated gravitational slope deformation), lat. 46,520805° long. 11,477532°, elevation 325 to 750 m a.s.l. (c) Landslide V58 (multiple rotational rock slide), lat. 46,611867° long. 11,542234°, elevation 475 to 850 m a.s.l.

2. Data and methods

2.1. Ancillary data and landslide features mapping

Topographic, geologic, and aerial photo datasets are freely available from the Province of Bolzano geoportal (Rete Civica Alto Adige, 2019). Topographic data of both landslides are available at a great level of detail thanks to the availability of a LIDAR digital elevation model (DEM) of the Province of Bolzano (2.5 m grid) surveyed in year 2005 and 1:5,000 scale topographic maps.

6

Geologic data of both landslide sites refer to the CARG geological map of Italy (a new updated version is currently being released, but is not yet publicly available). Aerial ortho-photos are available for many years, with the year 2014 being the most recent available dataset.

Landslide mapping in V58 and V70 was carried out by field surveys supported by aerial photos and shaded relief maps derived from the LIDAR DEM. Specifically, mapping was aimed at outlining the different landslide units and sub-units characterized by different types and the state of activity of the movements. Assessment of the state of activity was based on both field monitoring data (see next sections) and PS-SAR data (from ERS and ENVISAT satellites) available from the Italian National Geoportal (PCN, 2019).

2.2. Borehole coring

The litho-stratigraphy of the V58 and V70 landslides was reconstructed down to the bedrock on the basis of several continuous coring boreholes drilled between 1993 and 2012. In order to reduce the disturbance of soil and rock cores and define a detailed soil profile, vertical boreholes were drilled using a double tube core barrel with an inner diameter of 131 mm. At site V58, a total of 24 boreholes were drilled between 2006 and 2012 with an individual length varying between 22 and 210 meters (17 equipped with inclinometer tubes, 7 with piezometers). At site V70, a total of 30 boreholes were drilled between 1993 and 2012 with an individual length varying between 15 and 50 meters (16 equipped with inclinometer tubes and 11 with piezometers).

2.3. Inclinometric monitoring

As mentioned in paragraph 2.2, a total of 17 boreholes at site V58 and 16 boreholes at site V70 were equipped with inclinometer casings, a number of which were installed adjacent to the viaduct piers (Tombolato et al.; 2011; Simeoni et al., 2015). Inclinometric measurements from 1993 to 2013 in V70 and 2006 to 2013 in V58 were made available to the Authors by the E45 management company in raw data format, allowing checksum analysis and quantitative processing to be

7

performed (inclinometric plots subsequent to 2013, which show no significant changes in displacement rates, were on the other hand made available only as graphic files unsuitable for quantitative analyses). The four grooves were sampled using a biaxial probe and data processing was performed with four different approaches: a) using data from opposite grooves 1 and 3; b) using data from opposite grooves 2 and 4; c) using data from the four grooves measured by sensor A; d) using data from the four grooves measured by sensor B. The rationale of this approach was to check if the results would be the same irrespective of the processing methods used, so that systematic errors could be considered null. The four methods actually resulted in slightly different displacements cumulated from the bottom of the tube. As an example, Fig. 2 compares the y component of the displacements cumulated from the bottom in inclinometer I3 at site V70 by using grooves 1 and 3 or grooves 2 and 4. There was a difference of more than 8 mm at the ground surface (Fig. 2a). This difference did not diminish when measurements were corrected for systematic error due to instrument bias (Fig. 2b) or any other systematic error suggested by Mikkelsen (2003).
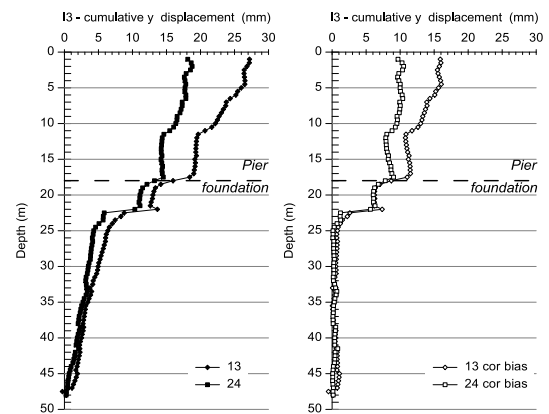

Fig. 2 − Inclinometer I3 at site V70. Component y of the cumulative displacement calculated with measurements on grooves 1-3 and grooves 2-4 from 25.6.2008 to 29.10.2009. a) processing without corrections; b) processing correcting error due to instrument bias.

In order to reduce the propagation of non-null systematic errors, inclinometer measurements were therefore cumulated at local depths only, i.e. over the depth intervals corresponding to significant

8

a)   b)

local displacements in all four processing methods. Details of the data processing and the effectiveness of this method are given in Simeoni and Ferro, 2015 and Simeoni and Puzzilli, 2017.

2.4. Piezometric monitoring

As mentioned in paragraph 2.2, a total of 7 boreholes at site V58 and 11 boreholes at site V70 were equipped with open standpipe and Casagrande piezometers (Tombolato et al.; 2011; Simeoni et al., 2015). Manual measurements were discontinuous in time (roughly on a six-monthly basis) from 1993 to 2013 in V70 and 2006 to 2013 in V58. The data were therefore suitable for determining the presence and average depth of groundwater only, but not to investigate the seasonality of water level changes or define detailed ground water distributions and their specific relationship with slope displacement rates. At site V70, 3 Casagrande piezometers were transformed into closed systems with automatic recording every 6 hours.

2.5. Total Station monitoring

In both the V58 and V70 landslides displacement of viaduct structures equipped with fixed target prisms was measured by Total Station monitoring on a roughly 3- or 4-monthly basis. Surveys in V70 were carried out from 2005 to 2013 using a Polar approach (installing the Total Station over a fixed pillar) and in V58 from 2008 to 2013 using the Free-station approach (since it was not logistically possible to build a fixed pillar). Total Station measurements showed seasonal variations with an amplitude of 5-6 mm, supposedly caused by refraction index changes, thus 2.5-3 mm may be assumed as a measure of Total Station monitoring accuracy (Simeoni and Ferro, 2015). The measurements were therefore re-processed in terms of yearly displacement rate.

2.6. Geotechnical laboratory testing

Disturbed samples of soils cored in boreholes were tested in the lab in order to determine grain size distribution, plasticity indexes and shear strength on reconstituted samples.

The grain size distribution was analysed up to a maximum size of 60 mm according to ASTM C136/C136M-14 (2014). Similar grain size distributions obtained from different samples were therefore added in order to obtain a larger significant sample size.

Consistency limits and plasticity indexes were obtained according to ASTM D4318-17.

Direct shear-box tests (consolidated-drained) were carried out on reconstituted specimens of 20 mm maximum height, including soil grain sizes smaller than 2 mm. After consolidation to the maximum vertical stress (ranging from 300 kPa and 600 kPa), samples were sheared to evaluate the strength at constant volume. Repeated shearing direction reversal cycles were then applied until the residual shear strength was attained.

2.7. *Slope stability back-analysis*

Two-dimensional slope stability analysis using Slope W (Geoslope, 2012) was carried out in representative cross sections of V58 and V70 with the Morgenstern-Price Limit Equilibrium Method. A back analysis approach was adopted in order to estimate the mobilized shear strength along possible sliding surfaces coherent with the improved geological model of the slopes. Back analysis assumed the groundwater conditions demonstrated by piezometric monitoring and null cohesion along sliding surfaces. The results returned the mobilized angle of friction φ' corresponding to a factor of safety equal to one. This was then compared to the shear resistance obtained in the laboratory.

2.8. *Crosscheck of results (redundancy and coherence checking)*

In order to strengthen the interpretation of slope movements, the accuracy of data processing and, more generally, the reliability of the information were crosschecked following the general operational framework shown in Fig. 3. The framework is based on two types of crosscheck tests: redundancy of data and coherence between different thematic information. The redundancy tests apply to similar physical quantities or characteristics (for example, displacement, soil type) and are

aimed at checking the agreement between measurements carried out with different instruments or between data collected with different types of investigation (e.g. field and laboratory investigations). Information passing the redundancy tests is therefore considered to be reliable and may be used to define and refine the geological and geotechnical models. Conversely, if the redundancy tests fail, more investigations, measurements or refinement of data-processing may be required. On the other hand, the coherence tests aim to validate the analysis results, including the geological and geotechnical models. For example, with reference to Fig. 3, data from monitoring that have passed the redundancy test are tested for coherence with respect to the geological model, and a no agreement result necessitates review of both the model and field measurements. On the other hand, if the geological model is coherent with the field monitoring results, then the field and laboratory investigations and testing are used to set up a geotechnical model that in turn is validated by means of back-analysis. If the geotechnical model and back-analysis results are not coherent, then the geotechnical model is reviewed on the basis of the geological model and, possibly, by extending the field and laboratory measurements and investigations. Conversely, if the geotechnical model and back-analyses results are coherent, then the model may be considered validated and may be used again to evaluate the potential effects on the slope of consolidation countermeasures such as deep-groundwater drainage or other engineering structures.
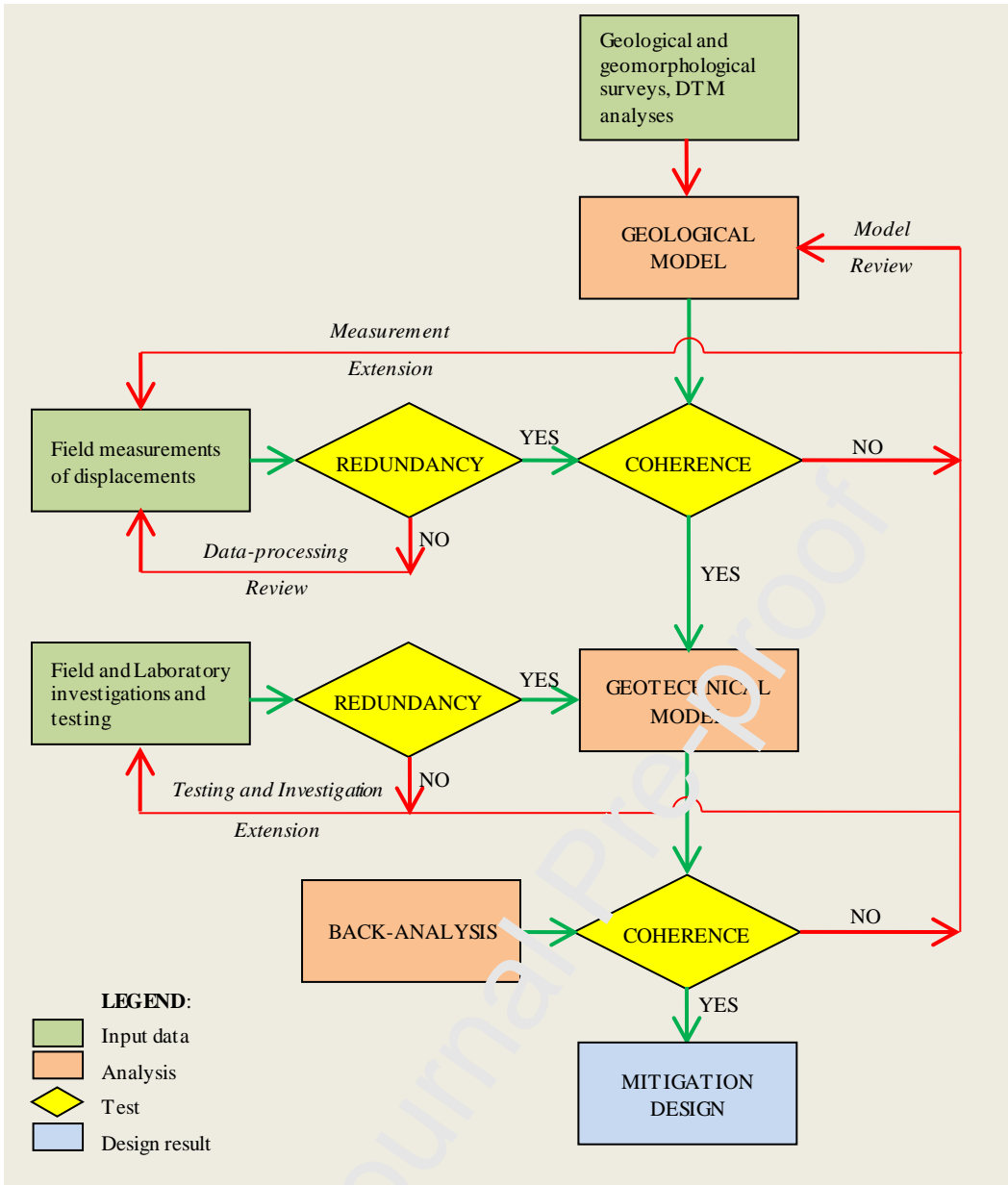
Fig. 3 – Framework for redundancy and coherence checking.

3. Results for V58 landslide

3.1. Landslide features mapping

Previous technical reports from the E45 highway management company considered the movements affecting Pier 7 to be caused by shallow rotational landslides localized in the lower part of the slope. However, mapping the slope considering a broader spatial perspective indicated that these phenomena must be set in the context of a large composite landslide affecting the metamorphic quartzphyllite at slope scale (Fig. 4). The landslide can be defined as a deep-seated retrogressive, multiple rotational rock slide (MRRS) in which two or more blocks have moved on curved sliding surfaces tangential to common deep surfaces of rupture (Erbacher and Clague, 1984). Toward the base of the slope, clay-rich surface deposits resulting from bedrock degradation are also affected by earth-slides. The overall slope movement extends over an area of 0.5 km^2, with a length of 800 m and a width of 700 m, a mean slope of 26° and a travel angle of 28°, for an estimated total MRRS volume in the order of 30 Mm^3. The inactive head scarp of the slide is located at 875 m a.s.l., along a NE-SW tectonic lineament, while another W-E lineament coincides with the right flank of the landslide. The lower limit of the landslide can be located below the Isarco river valley floor (on the basis of evidence from boreholes drilled at the toe of the slope). Furthermore, there are two secondary composite scarps within the landslide area at 750 m and 650 m, marking the limit between the upper, intermediate and lower blocks of the MRRS.
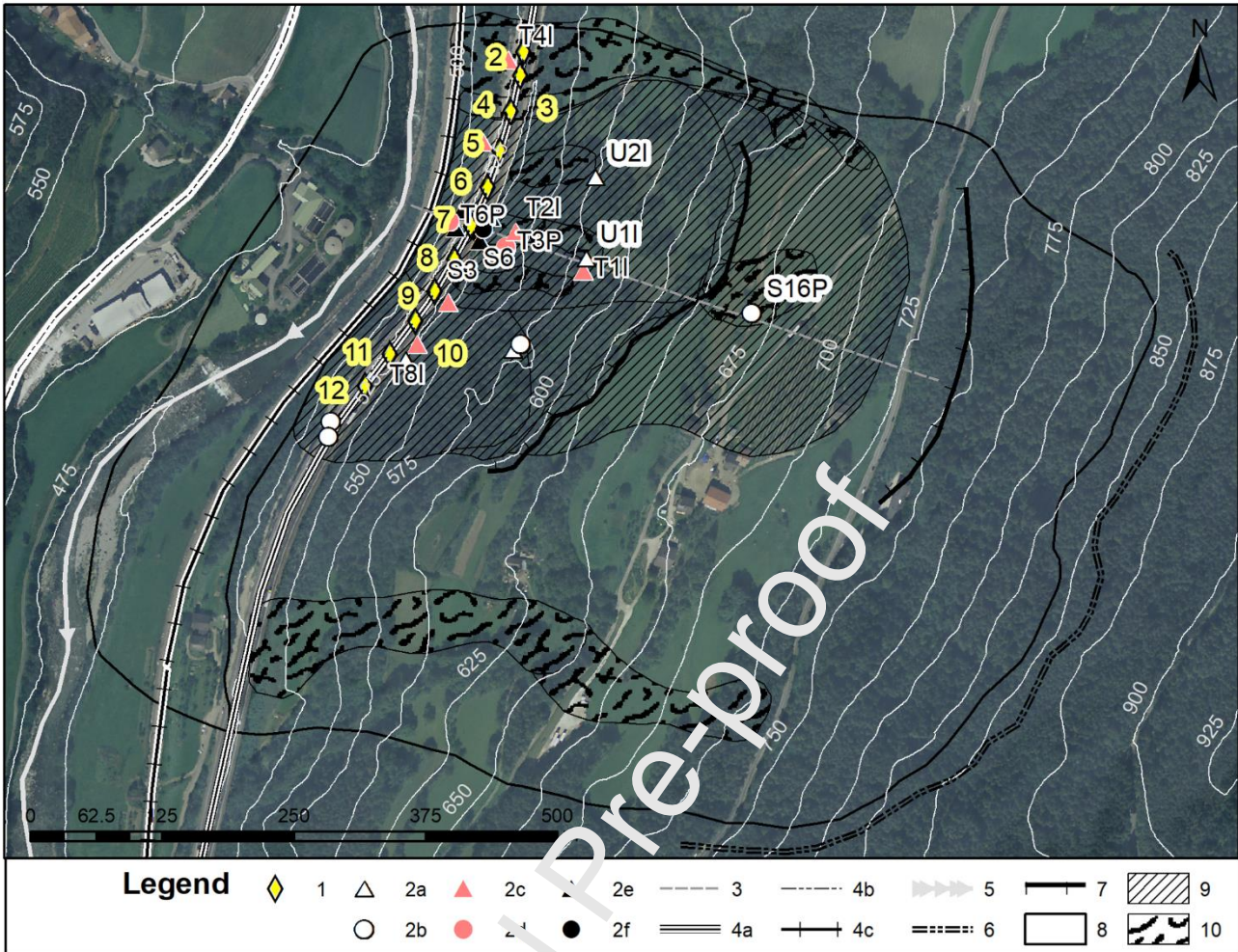
Fig. 4 – General map of landslide V58. Legend: 1: Pier, with number; 2: Drilling year and monitoring system, 2a: 2012, inclinometer; 2b: 2012, piezometer; 2c: 2008, inclinometer; 2d: 2008, piezometer; 2e: 2006, inclinometer; 2f: 2006, piezometer; 3: Cross-section trace; 4: 4a: Highway.4b: State Road; 4c: Railway; 5: Isarco River; 6: MRRS main scarp; 7: MRRS secondary scarp; 8: MRRS boundary; 9: Upper rock-slide boundary; 10: Earth-slide boundary.

3.2. Results and coherence of redundant monitoring systems

Installation of inclinometers and piezometers in V58 took place in 2006, 2008 and 2012 (Fig. 5), while Total Station monitoring started in 2008. The instrumented boreholes are mostly located along a cross section passing through Pier 7 of the viaduct, where deformation of the pads was first visually recognized, and Piers 3, 5, 9, 11 where deformations of the pads had in the meantime been identified by Total Station monitoring (Table 1). Boreholes reached depths of 40 m in 2006 (S3 and S6 in Fig. 4, around Pier 7), 210 m in 2008 (S16P, higher up on the slope, to install a piezometer) and 100 m in 2012 (U1I and U2I). Coarse soil was generally found in the uppermost meters, followed at greater depths by rock boulders and occasionally weathered rock in a matrix of coarse

14

soil and rarely with thin layers of fine soil covering the bedrock. Inclinometers indicated sliding surfaces at maximum depths of: -20 m close to Pier 7; max -31 to -48 m upslope Pier 7; max -24 m upslope Pier 5; max -34 m upslope Pier 9; max -47 m upslope Pier 11. Groundwater measurements in 10 open standpipe piezometers resulted in an average water table depth of 25 m from ground level (coherent with seepage parallel to the slope) with seasonal fluctuations in the order of +/- 4 m.
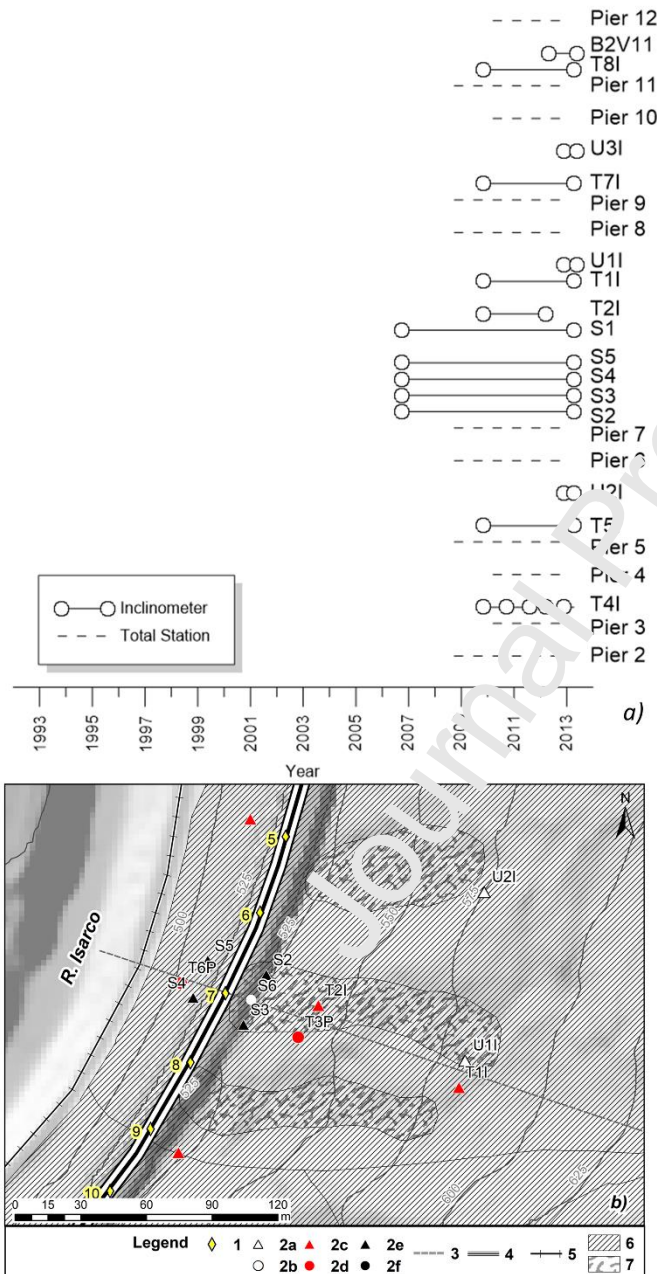

Fig. 5 – a) Field displacement measurement history at landslide V58: 2 or 3 measurements per year were carried out in the inclinometers, 3-4 measurements per year with the Total Station. b) Detail of the geological map around Pier 7. Legend: 1: Pier, with number; 2: Drilling year and monitoring system; 2a: 2012, inclinometer; 2b: 2012, piezometer; 2c: 2008, inclinometer; 2d: 2008, piezometer; 2e: 2006, inclinometer; 2f: 2006, piezometer; 3: Cross-section trace; 4: Highway; 5: Railway; 6: Upper rock-slide boundary; 7: Earth-slide boundary.

15

Total Station monitoring started in 2008 and was based on 4 surveys per year of two targets on each stem of piers 2 to 11; one target in the uppermost part of the stem, one target in the lower part. Multiple targets in each stem were distributed from the uppermost to the lowermost part. The measured displacements were always found to be higher in the lower targets, indicating a rigid backward roto-translation of the piers.

The mean yearly velocity recorded by the inclinometers and Total Station monitoring ranges between zero at Pier 3 and from 3.8 to 9.5 mm/year from Piers 5 to 11 (Table 1). This indicates that displacement rates increase from North to South. Inclinometer and Total Station results are quite similar at each pier (e.g. Pier 7 in Fig. 6), showing that redundant measurements are substantially coherent. Differences in mean displacements range between 10% (Pier 5) and 26% (Pier 9). It was also found that inclinometer T8I at Pier 11 had not measured displacements as it did not reach the sliding surface.

Viaduct Pier number	3	5	7	9	11
Inclinometer code	T4I	T5I	S3	T7I	T8I
Inclinometer displ. (mm/yr)	0	3.8	6.1	8.3	n.a.
Total Station displ. (mm/yr)	0	4.2	7.7	9.5	9.4

Table 1 – Mean yearly velocity at V58 landslide (data from 2010 to 2012)

Considering Pier 7 as an example (Fig. 6), displacements at inclinometers S3 and S4 were used to identify the single main sliding surface (SS1) located at about 5 to 10 m below the pier base (Fig. 6a) and, together with inclinometer S5, the linear displacement trends in the order of 3 to 7 mm/year (Fig. 6b). SS1 is considered as the present-day main active surface as it also extends below the neighbouring piles. Other sliding surfaces (such as the one at a depth of 3 m in Fig. 6a) are considered to be of minor relevance as they refer to shallow localized instability situations. As previously mentioned, Total Station displacements showed that the lower parts of the viaduct piers tend to suffer larger movements than the top parts. Assuming a linear trend from the top to the base of the pier, the displacement at the base of the pier foundations can therefore be estimated (Fig. 6c). This backward rotation of the piers can be ascribed either to the upper hinging effect of the E45

16

carriageway elements (the road deck represents a possible constraint on pier rotation), or to the predominant rotational kinematics of the local sliding surface. Estimated Total Station displacement at the base of pier 7, compared to inclinometer displacement for the period 2010-2012, shows that a substantially linear movement trend in the order of 7 mm/year is obtained by both monitoring systems (Fig. 6d).
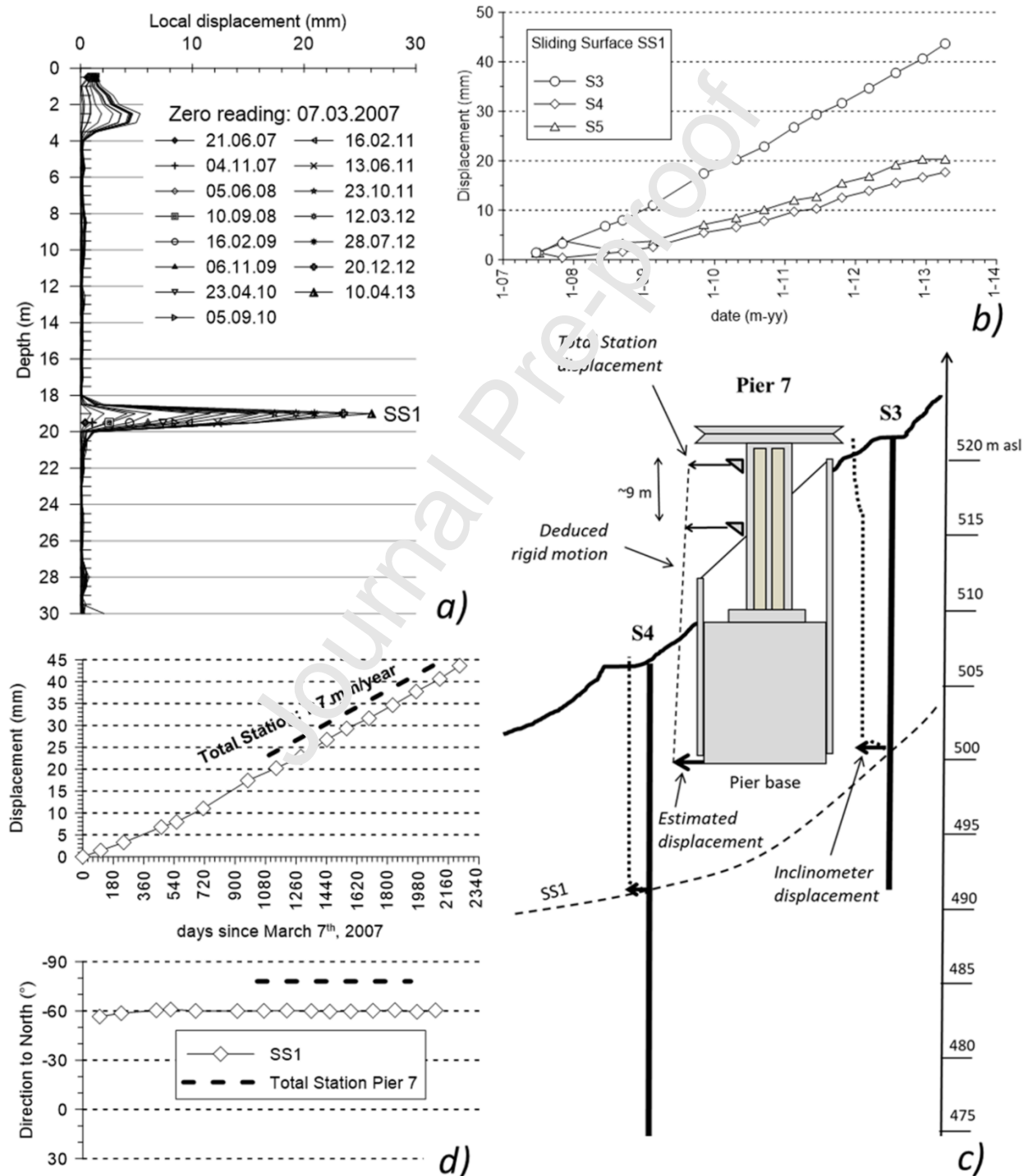
Fig. 6 –Redundancy of displacement measurements at Pier 7 of site V58; a) local displacements at inclinometer S3; b) displacement history of sliding surface SS1 at inclinometers S3, S4 and S5; c) sketch to compare inclinometer and Total Station displacements; d) inclinometer and Total Station displacement comparison.

3.3. Refined geological model

At the beginning of the study, displacements of Pier 7 were considered to be caused by a local rotational slide. The geological model of the slope was significantly refined on the basis of further and more accurate landslide mapping, together with borehole stratigraphy on sliding surfaces identified with a larger number of inclinometer and Total Station measurements. The cross section corresponding to Pier 7 (Fig. 7) can be considered as the most representative of the V58 landslide. On the basis of the stratigraphy of the deeper boreholes (i.. by considering the abrupt decreases of RQD or the presence of degraded fully softened layers in the rock masses), the inactive shear zone at the base of the slope-scale MRRS has been localized at a depth ranging from 100 m (in the medium-upper part of the slope) to a depth of 50 m (below the Isarco River bed). Overlying the main MRRS block, an active sliding surface separates it from an intermediate rock slide block. This surface outcrops at an elevation of 725 m a.s.l., where the slope has a well-defined scarp (Fig. 8b). Considering the borehole stratigraphy, this sliding surface corresponds to a specific layer particularly rich in silt and sparse angular rock fragments. At the toe of the slope, this active sliding surface runs at a depth of 3. m (inclinometer T2I), 19-20 m (inclinometer S3) and 13-15 m (inclinometer S4). Other curved sliding surfaces also divide the rock slide further into sub-units (Fig. 8b). Along the slope, one of these other shear surfaces outcrops at an elevation of 650 m a.s.l, while the other outcrops immediately above the Isarco River in the lower part of the slope.
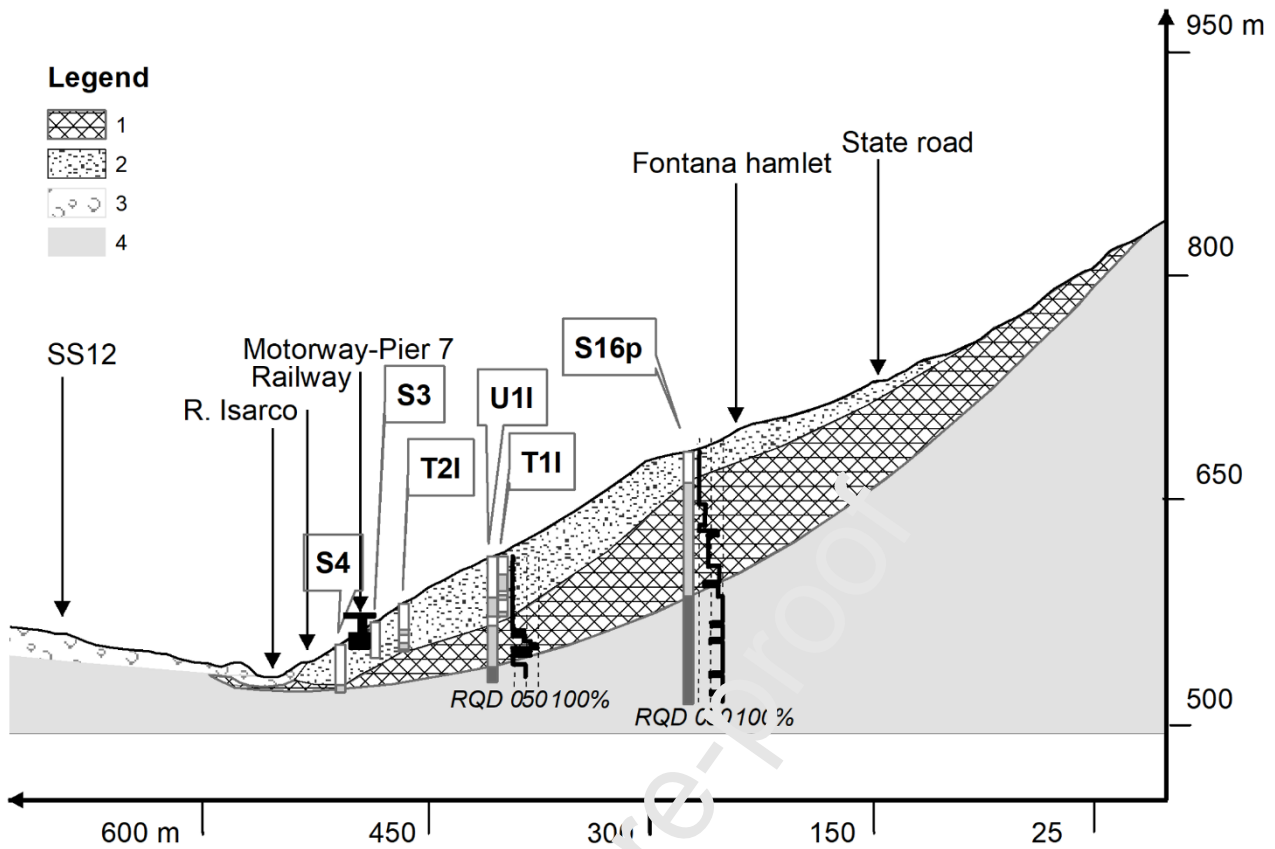
Fig. 7 – Cross section passing through Pier 7 of landslide V58. Note the borehole stratigraphy (white, deposit rich in matrix; grey, fractured rock; dark grey, bedrock) and RQD values. Legend:
1: MRRS body, mainly rock blocks; 2: MRRS body, mainly rock blocks in matrix; 3: Alluvial deposit; 4: bedrock.
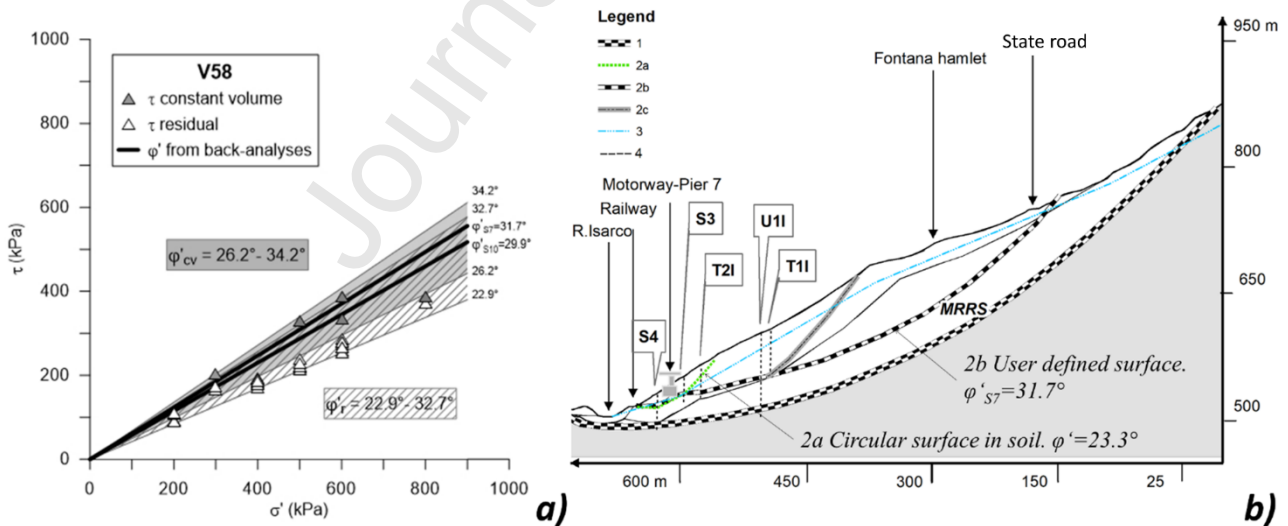

Fig. 8 – Landslide V58 (a) Shear strength from shear box tests and back-analyses. (b) cross-section passing through Pier 7: mobilized angles of shear resistance at the supposed sliding surfaces. Legend: 1: Main MRRS sliding surface; 2a: sliding surface analysed with equilibrium analysis and shear resistance not coherent with both the geological and geotechnical models; 2b: sliding surface analysed with equilibrium analysis and shear resistance coherent with both the geological and geotechnical models; 2c: sliding surface corresponding to the secondary scarp; 3: water table. The cross-section shows the pier and the underground stratigraphy (black continuous line).

3.4.   Refined geotechnical model and back analyses

19

The refined geological model was used as the basis for back analysis of stability conditions in order to define geotechnical units and sliding surfaces along which the mobilized shear strength was evaluated in comparison with the residual resistance determined by direct shear laboratory testing. Static groundwater conditions were considered in accordance with piezometric monitoring, which indicated a groundwater table subparallel to the slope located at 25 m from the ground.

The grain size distributions for landslide material at V58 are given in Fig. 9. Data refer to natural material and the finer part used for the reconstituted samples tested with the shear box. The soils are well graded and in general the grain size distribution of soils collected on the sliding surfaces was found to be not significantly different from that of the other soils, even when the finer part was selected for the shear box tests. The sample of sand (sample S4-C) collected at the toe of the slope and of alluvial origin was an exception. Neither did the soil differ in terms of plasticity, since in the plasticity chart all the soils lay between the A and U lines and between liquid limits of 20% and 29%.
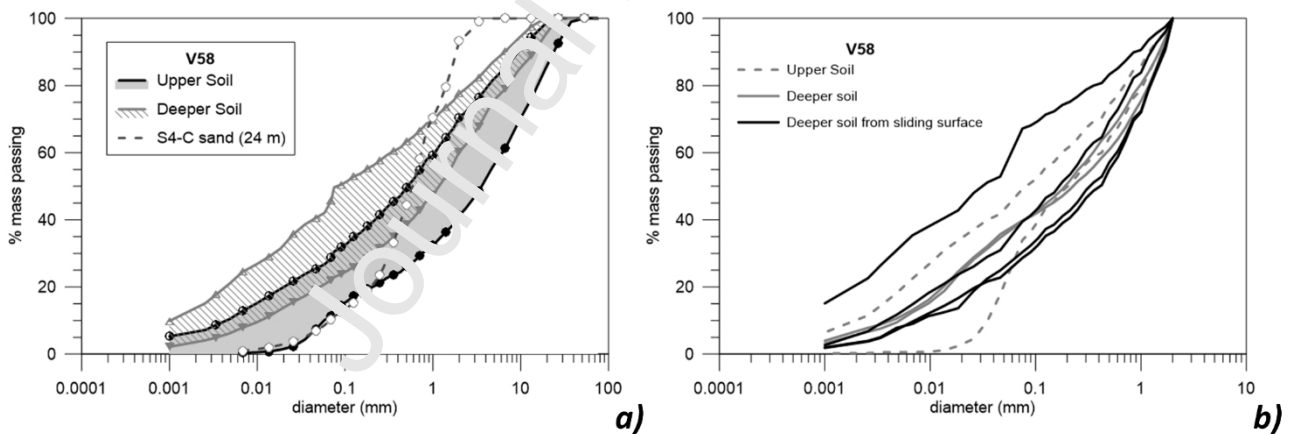

Fig. 9 – Landslide V58. Grain size distributions: a) natural soils; b) finer part used for the reconstituted samples tested with the shear box.

The results of the shear box tests (carried out with maximum vertical stresses ranging from 300 kPa to 600 kPa) are summarized in Fig. 8a. The friction angle varies through a fairly wide range of values: from 25.2° to 34.4° for the angle at constant volume; from 22.9° to 32.7° for the angle at residual strength. The decay from constant volume to residual conditions varies from 1.2° (equivalent to 4% of the resistance at constant volume) to 9.7° (33% of the resistance at constant

volume) with an average decay of 5.3° (18% of the resistance at constant volume). No significant relationships were found between decay and the clay fraction or plasticity of the samples.

A first back-analysis run was carried out according to the data collected before 2009. It considered a circular surface passing through the local displacement positions in inclinometers S3 and S5 and through the base of inclinometer S1; a factor of safety equal to one with an angle of shear resistance of 23.3° was obtained (Fig. 8b). However, this result shows at least two significant limitations: 1) if the sliding surface passed at the base of inclinometer S1, the length of the landslide would suggest a width involving at least the nearby piers and therefore further field investigation would be required; 2) the mobilized angle of shear resistance coincided with a lower limit of the angles of residual resistance obtained in the laboratory for the soil finer than 2 mm and this is unlikely, given that the soil in the field is very heterogeneous and well-graded and therefore a mobilized resistance close to the maximum values is to be expected.

Back-analyses were consequently repeated, taking into consideration the refined geological model found to be coherent with the redundant field measurements of displacements. Back analysis was carried out for sections passing through Pier 7 and through Pier 10, resulting in two different values ($\varphi'_{S7} = 31.7°$ and $\varphi'_{S10} = 29.9°$) for the mobilized angle of shear resistance. In Fig. 8a, these results for the actual mobilized angles of shear resistance are compared with the values obtained by the shear box tests. As might reasonably be expected, the mobilized angles of shear resistance fit with the lower boundary of the angles at constant volume and the upper boundary of the angles at residual strength. Since the back analysis provides coherent results, according to the methodological framework of Fig. 3, the entire dataset and models can be considered reliable.

4. Results for V70 landslide

4.1. Landslide feature mapping

Previous technical reports from the E45 highway management company considered the movements affecting piers 22 to 25 of the V70 viaduct to be caused by relatively shallow roto-translational

21

movements in the coarse scree-slope deposits covering the lower part of the slope. However, as in the previous case study, mapping the slope considering a broader spatial perspective indicated that these movements are to be considered in the framework of a much larger composite landslide affecting the Permian ignimbrites and tuffs at slope scale (Fig. 10). In this case, the landslide can be described as a deep-seated gravitational slope deformation (DSGSD) underlying the multiple rotational rock slide to the south, affecting the V70 viaduct and from which rock fall phenomena have led to the deposition of large scree fans at the base of the slope. A large inactive earth-slide also overlies the DSGSD in the northern sector.

The DSGSD has a total length of 800 m, a width of 600 m and a travel angle of approximately 30°. It covers an area of 0.4 km^2 and its volume is estimated at more than 30 Mm^3. The roughly triangular shape of the large scale DSGSD reflects the presence of two tectonic lineaments, oriented N-S and WNW-ESE. Borehole stratigraphy locate the upper limit of the phenomenon at 750 m a.s.l. in correspondence to a 50 m high arched scarp, and the lower limit at the Isarco valley floor. In the DSGSD area, infilled trenches, large downthrown rock blocks and uphill-facing scarps are also present. In the south-eastern sector, a sub-vertical scarp at 475 m a.s.l represents the upper limit of a deep rock slide. The multiple rotational rock slide body is affected by deep gullies through which the rock fall material is transported and deposited in a series of coalescent debris fans hosting the piers of the V70 viaduct.

Fig. 10 – General Map of landslide V70. Legend: 1: Pier, with number; 2: Drilling year and monitoring system; 2a: 2012, inclinometer; 2b: 2009, piezometer; 2c: 2009, inclinometer; 2d: 1993, piezometer; 2e: 1993, inclinometer; 3: Cross-section trace; 4: 4a: F45 highway; 4b: State Road 12; 5: Isarco River. 6: DSGSD scarp; 7: Rock-slide scarp; 8: DSGSD boundary; 9: Multiple Rock-slide boundary; 10: Earth-slide boundary; 11: Rock-fall deposit.

4.2.   Results and coherence of redundant monitoring systems

The inclinometers and piezometers in V70 were installed progressively from 1993 to 2012, while Total Station monitoring started in 2004 (Fig. 11a). The boreholes are located at the toe of the slope, mainly next to the piers with the exception of inclinometers T2I, T5I and U3I, located along the eastern side of the State Road, close to the River Isarco (Fig. 11b). In the boreholes, coarse soil was found in the uppermost meters, while at greater depths boulders of rock, occasionally weathered

23

rock, in a matrix of coarse soil and rarely with thin layers of fine soil were cored down to the bedrock. The inclinometers identified multiple sliding surfaces in the northern part of the DSGSD (at T1I, I2, I3 and I6, Simeoni et al., 2015): an upper sliding surface was identified at the base of the pier foundations at depths ranging from 16 to 24 m (the so-called "foundation sliding surface", accounting for most of the displacements), another secondary sliding surface was identified 5-7 m lower (the so-called "deep sliding surface"). At inclinometers T3I, T4I and T6I in the southern part of the landslide, only the "deep sliding surface" was identified. Inclinometers installed between the State Road and the river (T2I and T5I) did not detect displacements.

Groundwater measurements since 2009 were based on 4 Casagrande piezometers installed in boreholes T8P and T9P (3 of which were transformed into closed-system piezometers with automatic recording by pushing pressure transducers into the filters). When total heads were higher than the river elevation (at 336 m a.s.l.), there was seepage down the slope. This was reversed in certain periods, so that episodic seepage from the river to the slope can be supposed. In all these cases, however, the water table always remained below the sliding surface. Stability back-analysis was therefore carried out considering no groundwater above the sliding surfaces.

Total Station monitoring started in 2004 and was based on 3 surveys per year of three targets on the stem of piers 22 to 25 and four targets on the stem of pier 26. Multiple targets in each stem were distributed from the uppermost to the lowermost part. The measured displacements were always found to be higher in the lower targets, indicating a rigid backward roto-translation of the piers.

The mean yearly velocity recorded by the inclinometers and Total Station monitoring ranges from 6.7 to 10.1 mm/year over adjacent Piers 22 to 26 (Table 2). This indicates that displacement rates are quite uniform from North to South. The inclinometer and Total Station results are quite similar at most piers, showing that the redundant measurements are substantially coherent. The differences are very limited at Pier 22 (9%), Pier 23 (5%) and Pier 25 (4%), larger at Pier 24 (26%) and significant at Pier 26 (43%, in this case, the discrepancy can be attributed to the fact that the

24

inclinometer closer to the pier was not installed properly and comparison with the Total Station therefore refers to an inclinometer placed at quite a distance from the pier).

Considering Pier 24 as an example (Fig. 12), displacements at inclinometer I3 (Fig. 12a) were cumulated from 15.5 m to 18.5 m at the foundation sliding surface (surface SS1), and from 21.0 to 21.5 m at the deep sliding surface (surface SS2). Over the years, three different inclinometer probes were used to carry out periodic monitoring, making data continuity impossible (Fig. 12b). Moreover, readings from probe 3 were of poor quality since the checksums were not completely constant along depth and the inclinometer displacements from probe 3 were not therefore compared with the topographic displacements. As previously mentioned, Total Station displacements showed that the lower parts of the viaduct piers tend to suffer larger movements than the top parts (Fig. 12c). Considering a linear trend from the top to the base of the pier, the displacement at the base of the pier foundations can therefore be estimated (Fig. 12c). This backward rotation of the piers can be ascribed either to the upper hinging effect of the E45 carriageway elements (the road deck represents a possible constraint on pier rotation), or to the predominant rotational kinematics of the local sliding. Estimated Total Station displacement at the base of pier 24 compared to inclinometer displacements (i.e. the sum of the deep sliding surface and the foundation sliding surface) for the period 2008-2010 shows that a substantially linear movement trend in the order of 10 mm/year is obtained by both monitoring systems (Fig. 12d).
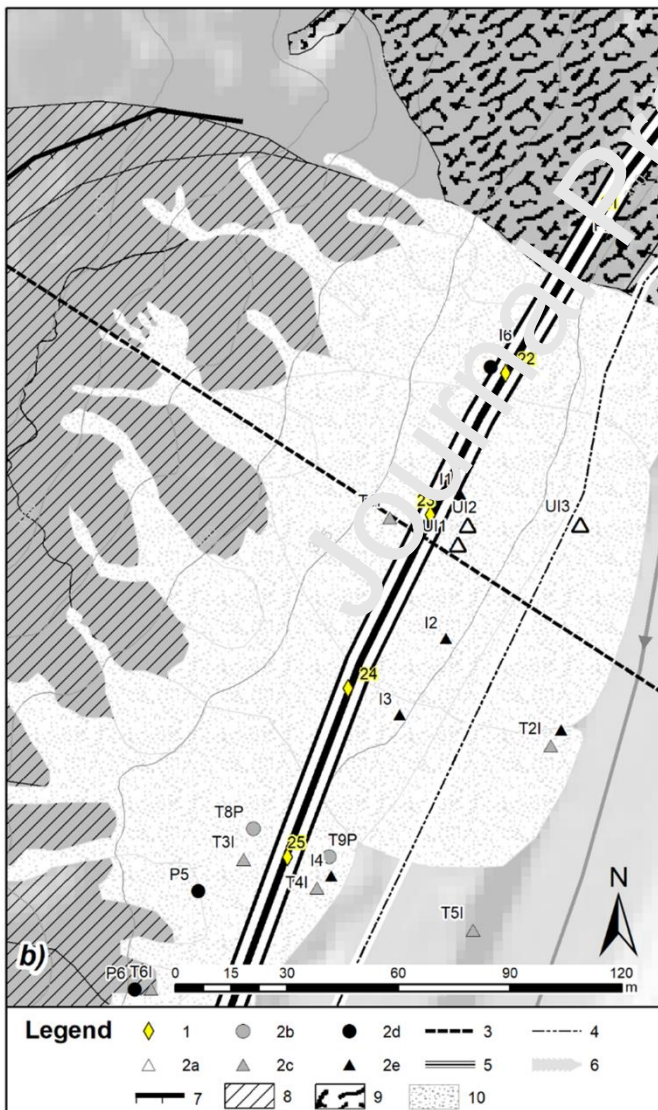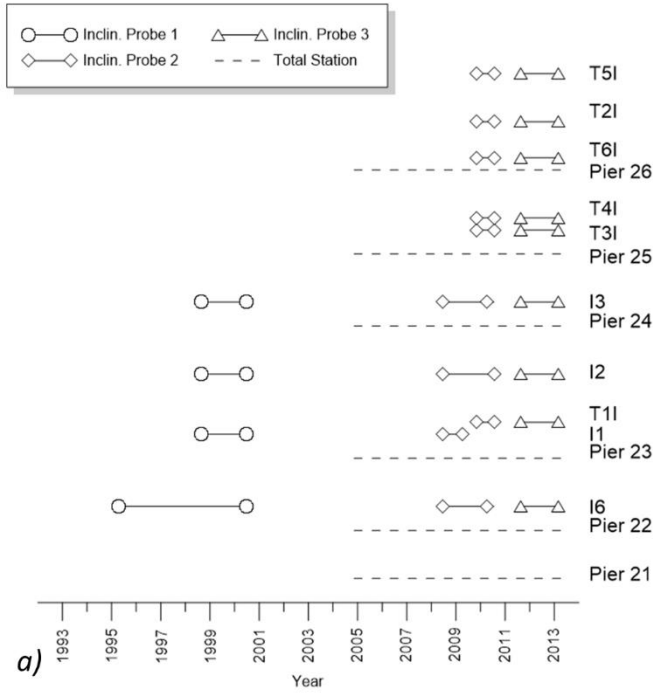
Fig. 11 – Landslide V70. a) Field displacement measurement history at landslide V70: the frequency of inclinometer measurements varies from 1/month in 1995 to 2/year in 2009 and 2010, Total Station measurements were carried out

26

on a 3-monthly base. b) Detail around landslide toe. Legend box b): 1: Pier, with number; 2: Drilling year and monitoring system; 2a: 2012, inclinometer; 2b: 2009, piezometer; 2c: 2009, inclinometer; 2d: 1993, piezometer; 2e: 1993, inclinometer; 3: Cross-section trace; 4: State Road 12; 5: Motorway; 6: Isarco River 7: Rock-slide scarp; 8: Multiple Rock-slide boundary; 8: Earth-slide boundary; 9: Rock-fall deposit.

Viaduct Pier number	22	23	24	25	26
Inclinometer code	I6	T1I	I3	T3I	T6I
Inclinometer displ. (mm/yr)	8.2	8.6	10.1	8.9	6.7
Total Station displ. (mm/yr)	7.5	8.2	8.0	9.3	9.6

Table 2 Mean yearly velocity at V70 landslide (data from 1993 to 2012)
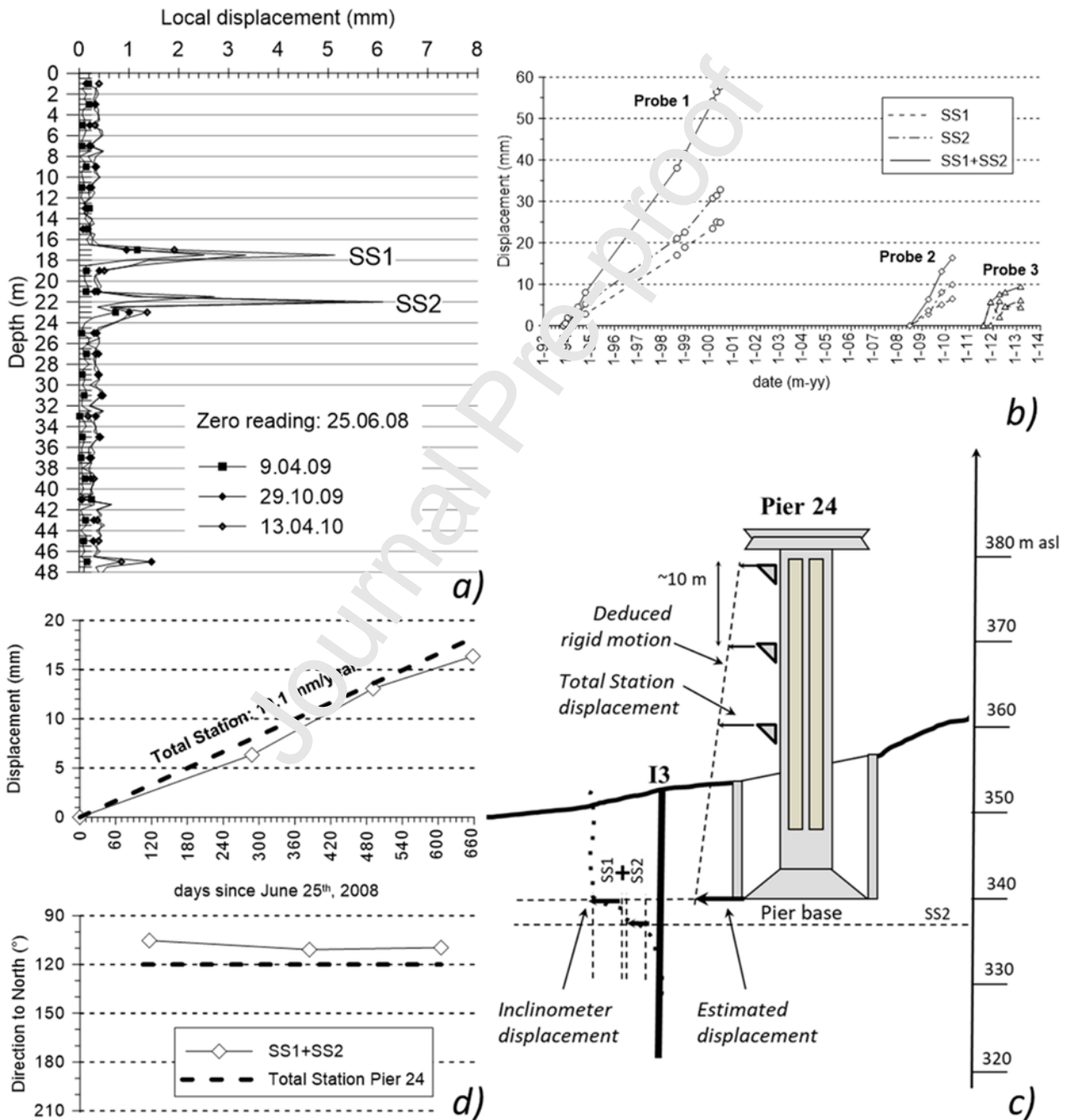

Fig. 12 – Redundancy of displacement measurements at Pier 24 of site V70; a) local displacements at the inclinometer I3; b) displacement history at the two sliding surfaces; c) sketch to compare inclinometer and Total Station displacements, d) inclinometer and Total Station displacement comparison.

27

4.3. Refined geological model

At the beginning of the study, subsurface displacements at the piers were thought to be the result of localized movements affecting the coarse deposits of the debris fans. The geological model of the slope can now be significantly refined on the basis of landslide mapping, borehole stratigraphy and the sliding surfaces identified with a larger number of inclinometers and measurements. The cross section corresponding to Pier 23 (represented in Fig. 13) can be considered as the most representative of the V70 landslide. The inclinometers highlight active sliding surfaces at different depths inside the debris fans: from 16 m to 22 m, the so-called "foundation sliding surface" accounting for most of the displacements; around 4 m deeper, the so-called "deep sliding surface". This deep surface has been interpreted as probably connected with the active movements of the rockslides. However, since inclinometers installed between the State Road and the river (T2I and T5I) did not detect displacements, all the sliding surfaces must outcrop above the State Road. This key factor was specifically considered while carrying out back analysis of stability conditions.
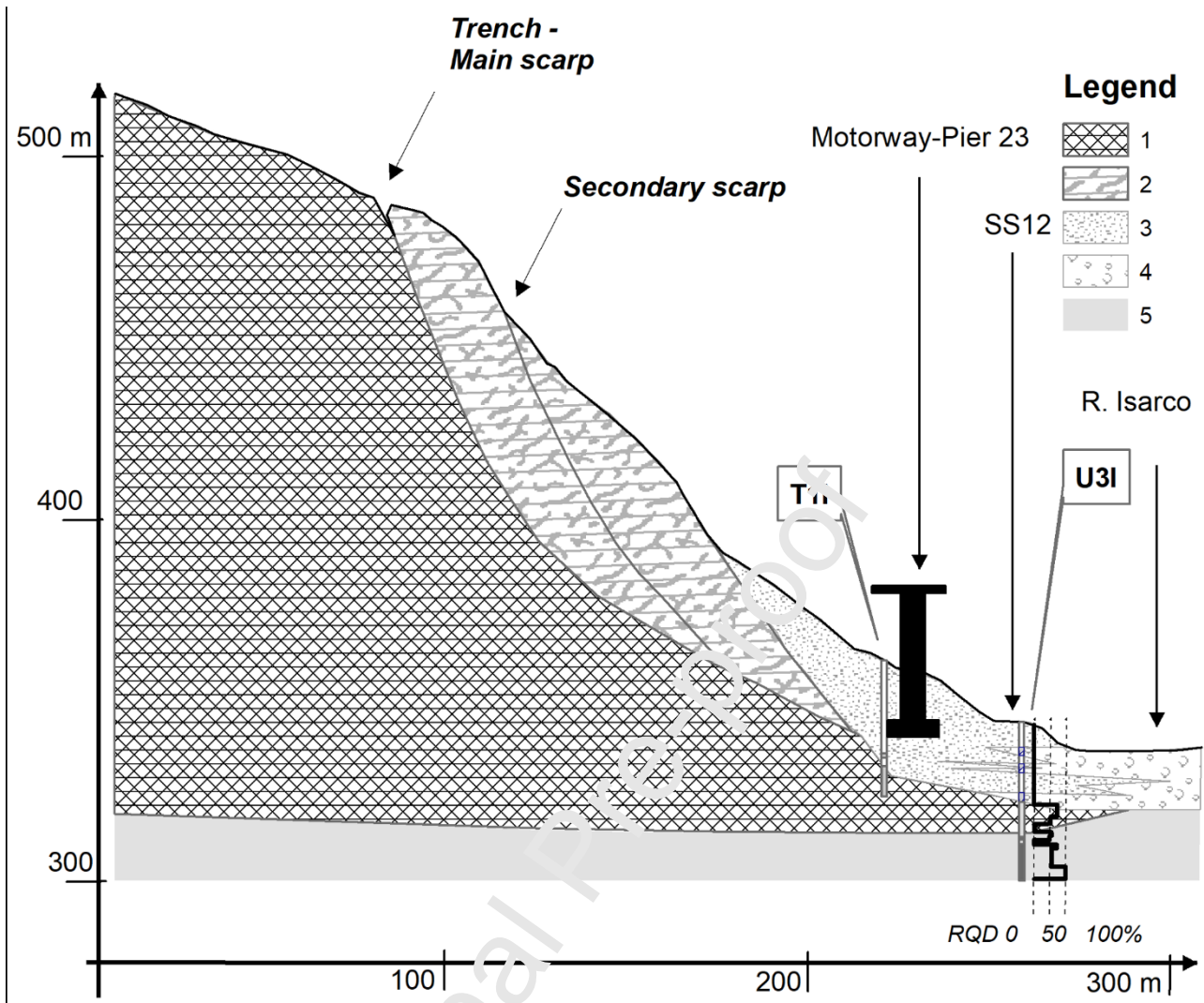
Fig. 13 – Landslide V70. Cross section passing through Pier 23 of landslide V70. The cross-section shows the pier, the borehole stratigraphy (white, deposit rich in matrix; grey, fractured rock; dark grey, bedrock and the RQD distribution. Legend: 1: DSGSD body; 2: Multiple Rock-slide body; 3: Debris fan from rock-falls; 4: Alluvial deposit; 5: bedrock.

4.4. Refined geotechnical model and back analyses

The refined geological model was used as the basis for back analysis of stability conditions in order to define the geotechnical units and sliding surfaces along which mobilized shear strength was evaluated in comparison with the residual resistance determined by direct shear laboratory testing. An absence of groundwater above the sliding surfaces was considered, in accordance with piezometric monitoring indicating total heads in the debris fan deposits lower than the sliding surfaces. The grain size distributions for landslide material at V70 are summarized in Fig. 14. Data refer to natural material and the finer part used for the reconstituted samples tested with the shear

29

box. Except for some levels of sand or sand with silt, collected at the toe of the slope and of alluvial origin, the soils are well graded, although the uppermost soils are generally coarser than those collected at deeper locations, in some cases, produced by the weathering of rock boulders. The maximum clay fraction in natural soils was about 10%, while in samples tested with the shear box the clay fraction ranges from 10 to 20%. Soils collected on the sliding surfaces did not generally differ significantly from other samples. No differences in plasticity were found, since in the plasticity chart all samples lay between the A and U lines and between the liquid limits of 21% and 33%.
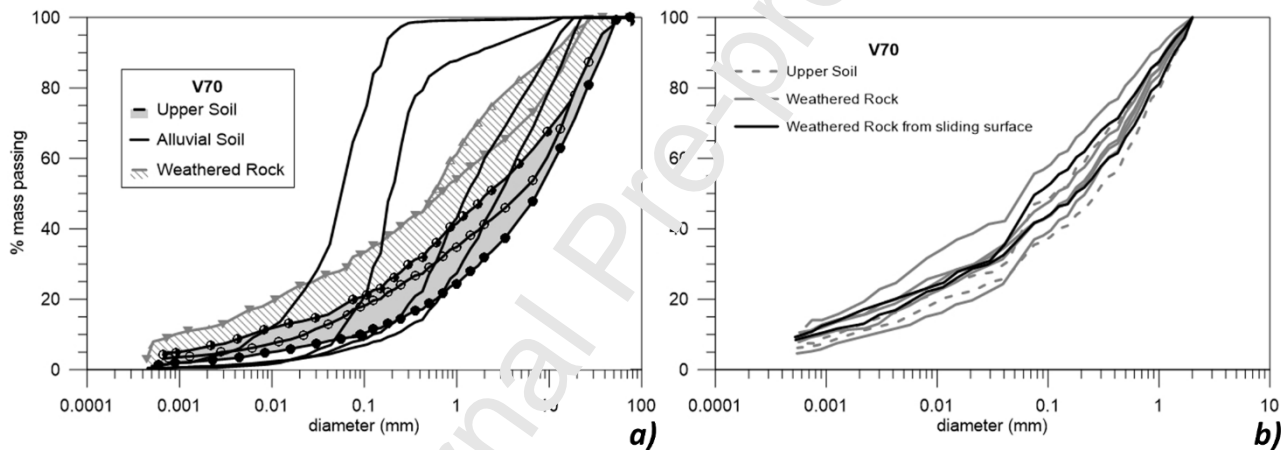

Fig. 14 – Landslide V70. Grain size distributions: a) natural soils; b) finer part used for the reconstituted samples tested with the shear box.

The results of the shear box tests (carried out with maximum vertical stresses ranging from 200 kPa and 600 kPa) are summarized in Fig. 15a. The friction angle varies through a fairly wide range of values: from 26.2° to 34.2° for the angle at constant volume and from 21.1° to 29.7° for the angle at residual strength. The decay from constant to residual volume varied from 0.9° (equivalent to 9% of the resistance at constant volume) to 12.4° (43% of the resistance at constant volume) with an average decay of 5.1° (18% of the resistance at constant volume). No significant relationships were found between decay and the clay fraction or plasticity.

The back-analysis runs considered three different hypotheses for the geometry of the sliding surface, each coherent with the geomorphological profile of the slope. Hp 1 considers a circular

30

sliding surface developing entirely in the debris fan soils only. Hp 2 assumes a sliding surface in the rockslide up to the secondary scarp. Hp 3 assumes a sliding surface in the rockslide up to the main scarp (Simeoni et al., 2015). The corresponding mobilized angles of shear resistance φ'_{S1} (for the soil), φ'_{R2} and φ'_{R3} (for the rock) are summarized in Fig. 15b. These values can reasonably be considered as residual shear strength values for both the soil and the rock mass. The fact that the mobilized angle in the multiple rock sliding surfaces is lower in the deeper surface (29.9°) that in the intermediate surface (31.4°), is in agreement with the evidence of a more evolved trench connected to the main scarp.
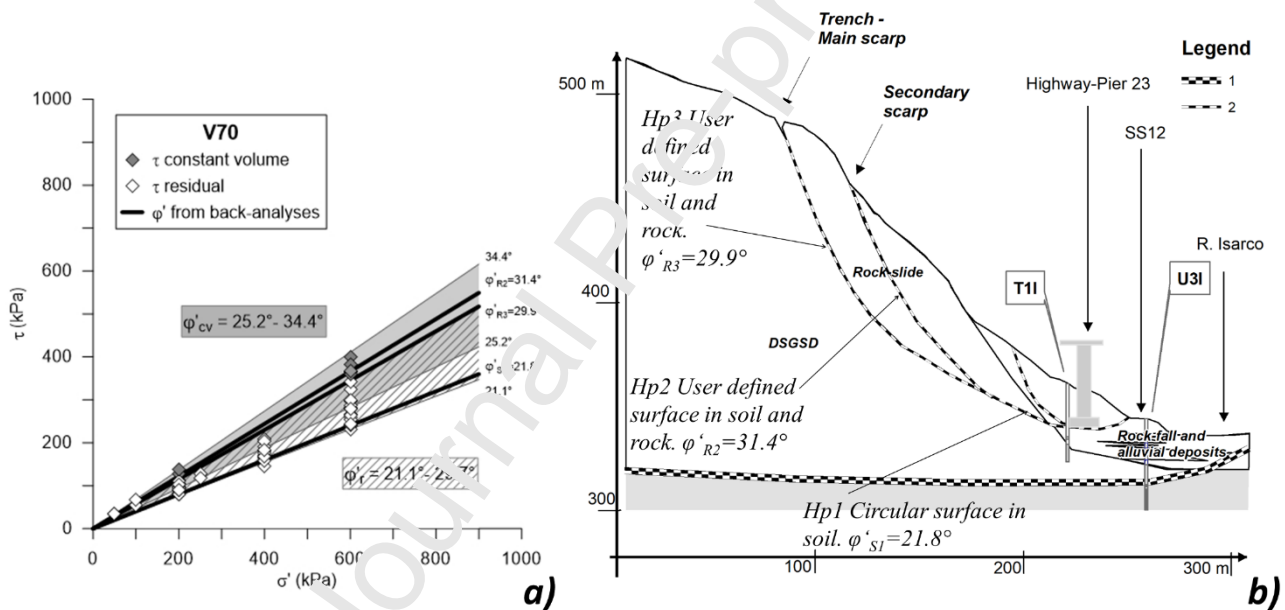

Fig. 15 – Landslide V70. a) Shear strength from shear box tests and from back-analyses. b) cross-section passing through Pier 23: mobilized angles of shear resistance for the three different sliding surface hypotheses. Legend: 1: DSGSD supposed share zone; 2: Sliding surface analysed with equilibrium analysis.

5. Discussion and conclusions

Based on the results obtained in this study, the discussion should consider both specific findings at the V58 and the V70 landslides as well as more general issues.

Displacement monitoring of the V58 and V70 landslides revealed steady-state linear displacement trends (Fig. 6 and Fig. 12) in the order of a maximum of 10 mm/year (type I in the classification by

Cascini et al., 2014), a trend similar to that of other extremely-slow landslides (Glastonbury and Fell, 2008). In V58, the geological model has been thoroughly revised with respect to the extremely simplified model considered initially. The revised model envisages the existence of a multiple rotational rock slide extending at slope scale, involving a total of 30 Mm^3 of rock masses and slope debris. Our results indicate that the displacements suffered by the V58 viaduct over a stretch of about 400 m (from Pier 5 to Pier 11), can actually be related to a specific active rock slide unit of about 6 Mm^3 in volume. This unit moves at a maximum rate of 9.5 mm/year on sliding surfaces which extend from a secondary scarp located at an elevation of 750 m a.s.l. to the base of the viaduct without involving the railway located at the toe of the slope. In V70, our results again led to a through revision of the geological and geotechnical models. The movements affecting the highway viaduct over a stretch of 200 m (from Pier 22 to Pier 26), are now ascribed to the activity of a retrogressive rock slide unit of about 1 Mm^3, developing in the frontal portion of a much larger and previously unrecognised 33 Mm^3 deep-seated gravitational slope deformation. The active sliding surfaces of the retrogressive rock slide move at a maximum rate of 10.1 mm/year entirely below the pier foundations (Piers 25 and 26) or, alternatively, both below and at the base of the pier foundations (Pier 22 to Pier 24). The evidence gathered at the V70 and V58 landslides, characteristics of the structure of the viaducts and record of past structural maintenance indicate that, in principle, the E45 viaducts can tolerate the extremely-slow displacement rates of the analysed landslides, providing periodic structural remediation measures are adopted (indicatively every 20 years in V70 and every 40 years in V58). On the basis of the geotechnical models validated in this study, possible measures to increase the factor of safety and reduce the displacement rate can nevertheless now be identified. At site V58, where the active sliding surfaces develop mainly below the groundwater table, the factor of safety can be increased by lowering the hydraulic heads with subsurface drainage systems. Preliminary stability analyses show that the factor of safety should increase by approximately 1% for each meter a water table modelled parallel

to the slope is lowered. Conversely, at site V70, where the active sliding surfaces develop mostly above the water table, the factor of safety can be increased only by toe-buttressing.

Study of the V58 and the V70 landslides also highlights some issues of more general relevance. The first issue concerns identification of extremely slow landslides during the design of transport infrastructures. The large extension and composite nature of these types of landslides might, in fact, not be recognised if the area investigated during geotechnical design is limited to the immediate surroundings of the structure to be built. V58 and the V70 are paradigmatic examples, as they were not identified during highway design and construction and, even when damage to the viaducts appeared, they were at first interpreted in relation to localized slope instability phenomena, and not to large composite slope-scale landslides.

A second issue regards the fact that even if the geomorphological evidence of large-scale landslides is recognized, assessment of their displacement rate is problematic, given that movements below 10 mm/year are likely to be masked or biased by errors in the monitoring systems adopted. In this study, precise assessment of the extremely slow displacement rates affecting the V58 and V70 slopes was possible only through adoption of multi-method long-term site-specific monitoring and specific data processing precautions. To minimise error propagation over the entire length of the inclinometer tubes, measurements were carefully verified by checksums and it was nevertheless beneficial to integrate incremental displacements locally, i.e. across each specific sliding surface recognized. At the same time, Total Station results were assessed as averaged yearly displacement rates only, to rule out biased measurements affected by residual random errors.

A third issue concerns the role of back-analysis of slope stability conditions in large-scale composite landslides, in which the extension and shape of the sliding surfaces is inevitably extrapolated on the basis of pointwise information and the geotechnical model is inevitably a simplification of the slope conditions. Since the factor of safety of active extremely slow landslides must necessarily be close to unity, back-analysis can nevertheless make it possible to assess whether the mobilized shear strengths required for limit equilibrium along the identified sliding

surfaces are coherent with the strength parameters obtained in laboratory tests. If this is not the case, then the geological-geotechnical models should probably be revised as they are somehow in contrast with basic physical principles. Once the geotechnical model has been validated by back-analysis, it can also be exploited to analyse possible solutions to increase the factor of safety and mitigate slope instability.

In conclusion, it should also be stressed that in extremely slow landslides, monitoring and modelling results should be considered validated only if data from different monitoring systems and analysis techniques prove reciprocally consistent. In the cases of the V58 and V70 landslides, a great deal of investigation, monitoring and analysis, together with meticulous cross-checking of data consistency, was required in order to define the deep-seated, extremely slow landslides. As a result, the two landslides were finally included in the natural hazards database of the local administrations (Rete Civica Alto Adige, 2019) and the slope-instability mitigation programme of the E45 highway management company.

References

ASTM, 2014. Sieve Analysis of Fine and Coarse Aggregates, ASTM C136/C136M-14, Annual Book of ASTM Standards, American Society for testing and materials, West Conshohocken, United States.

ASTM, 2017. Standard Test Methods for Liquid Limit, Plastic Limit, and Plasticity Index of Soils, ASTM D4318-17, Annual Book of ASTM Standards, American Society for testing and materials, West Conshohocken, United States.

Bidwell, A., Cruden, D., Skirrow, R., 2010. Geohazard Reviews of Highway Corridors Through Mountainous and Foothills Terrain, Southwestern Alberta. Proc. of the 63 Canadian Geotechnical Conference, Calgary, Vol. 1.

Cascini, L., Calvello, M., Grimaldi, G.M., 2014. Displacement Trends of Slow-moving landslides: Classification and Forecasting. Journal of Mountain Science 11(3), 592-606. DOI: 10.1007/s11629-013-2961-5.

Cascini L., Fornaro G. and Peduto D. (2010). Advanced low- and full-resolution DInSAR map generation for slow-moving landslide analysis at different scales. Engineering Geology, 112 (1-4): 29-42. doi:10.1016/j.enggeo.2010.01.003

Carey, J. M., Moore, R., Petley, D., Siddle, H. J. (2007). Pre-failure behaviour of slope materials and their significance in the progressive failure of landslides. Landslides and Climate Change: Challenges and Solutions (McInnes, R., Jakeways, J., Mathie, E. eds); Taylor & Francis Group: London, UK, 207-215.

Cohen-Waeber, J., Sitar, N., Bürgmann, R., 2013. GPS instrumentation and remote sensing study of slow moving landslides in the eastern San Francisco Bay hills, California, USA. Proc. of the 18th International Conference on Soil Mechanics and Geotechnical Engineering, Paris, September 2-6 2013, 2169-2172.

Corominas, J., Iglesias, R., Aguasca, A., Mallorquí, J.J., Fàbregas, X., Planas, X., Gili, J.A., 2014. Comparing Satellite Based and Ground Based Radar interferometry and field observations at the Canillo landslide (Pyrenees). Engineering Geology for Society and Territory. Vol. 2: Landslides and Processes, 333-337. Doi: 10.1007/978-3-319-09057-3_51.

Corsini A., Farina P., Antonello G., Barbieri M., Casagli N., Coren F., Guerri L., Ronchetti F., Sterzai P., Tarchi D. (2006) Space-borne and ground-based SAR interferometry as tools for landslide hazard management in civil protection. International Journal of Remote Sensing, 27 (12), 2351–2369.

Crosta, G.B., Chen, H. and Lee, C.F. (2004) Replay of the 1987 Val Pola Landslide, Italian Alps, Geomorphology 60 (1–2), 127–146.

Crosta, G. B., Frattini, P., & Agliardi, F. (2013). Deep seated gravitational slope deformations in the European Alps. Tectonophysics, 605, 13-33.

Cruden, D.M., Varnes, D.J., 1996. Landslides Types and Processes. In: Turner AK, Schuster RL (eds). Landslides: investigation and mitigation (Special Report). Washington, DC, USA: National Research Council, Transportation and Research Board Special Report 247, 36–75.

Di Maio, C., Vassallo, R., Vallario, M., Pascale, S., Sdao F., 2010. Structure and kinematics of a landslide in a complex clayey formation of the Italian Southern Apennines. Engineering Geology 116, 311–322. doi: 10.1016/j.enggeo.2010.09.012.

Eisbacher, G.H. and Clague, J.J. 1984 Destructive mass movements in high mountains: hazard and management. Paper 84-16. Geological Survey of Canada, Ottawa, Ontario, 230pp.

Fenti, V., Silvano, S., Spagna, V., 1977. Rockfalls in the Isarco Valley (South Tyrol) and proposed methods for a "provisional map". ISMES, 90, Bergamo (Italy).

Flageollet, J-C., 1996. The time dimension in the study of mass movements. Geomorphology, 15, 185-190.

Geoslope, 2012. Stability Modeling with SLOPE/W An Engineering Methodology July 2012 Edition GEO-SLOPE International Ltd. 238pp. available online. http://downloads.geo-slope.com/geostudioresources/8/0/6/books/slope%20modeling.pdf?v=8.0.7.6129

Glastonbury, J., Fell., R., 2008. Geotechnical characteristics of large slow, very slow, and extremely slow landslides. Canadian Geotechnical Journal 45, 984–1005. doi:10.1139/T08-021.

Longoni, L., Papini, M., Brambilla, D., Arosio, D., & Zanzi, L. 2016. The role of the spatial scale and data accuracy on deep-seated gravitational slope deformation modeling: The Ronco landslide, Italy. Geomorphology, 253, 74-82.

Macfarlane, D.F., 2009. Observations and predictions of the behaviour of large, slow-moving landslides in schist, Clyde Dam reservoir, New Zealand. Engineering Geology 109, 5–15. doi:10.1016/j.enggeo.2009.02.005

Macciotta, R., Martin, C.D., Morgenstern, N.R., Cruden D.M., 2015. Development and application of a quantitative risk assessment to a very slow moving rock slope and potential sudden acceleration. Landslides. Doi: 10.1007/s10346-015-0609-y.

Mansour F.M., Morgenstern, N.R., Martin, C.D., 2011. Expected damage from displacement of slow-moving slides. Landslides 8, 117–131 Doi: 10.1007/s10346-010-0227-7

Mikkelsen, P.E., 2003. Advances in inclinometer data analysis. Proc. of the 6th International Symposium on Field Measurements in Geomechanics, Oslo, Norway, September, 15-18 2003, 555-567.

Noferini, L., Pieraccini, M., Mecatti, D., Macaluso, G., Atzeni, C., Mantovani, M., Marcato, G., Pasuto, A., Silvano, S., Tagliavini, F., 2007. Using GB-SAR technique to monitor slow moving landslide, Engineering Geology - ENG GEOL. doi:10.1016/j.enggeo.2007.09.002

Palis, E., Lebourg T., Tric, E., Malet, J.P., Vidal, M., 2017. Long-term monitoring of a large deep-seated landslide (La Clepiere, South-East French Alps): initial study. Landslides 14, 155-170. Doi: 10.1007/s10346-016-0705-7.

Puzrin, A.M., Schmid, A., 2012. Evolution of stabilised creeping landslides. Géotechnique 62(6), 491–501. Doi: 10.1680/geot.11.P.041.

Raspini, F., Bianchini, S., Ciampalini, A., Del Soldato, M., Solari, L., Novali, F., Del Conte, S., Rucci, A., Ferretti, A., Casagli, N., 2018. Continuous, semi-automatic monitoring of ground deformation using Sentinel-1 satellites. Sci. Rep. 8, 7253. doi:10.1038/s41598-018-25369-w

Rete Civica Alto Adige, 2019. Geoportale Alto Adige. http://geoportale.retecivica.bz.it

PCN, 2019. Portale Cartografico Nazionale – Ministero dell'Ambiente. http://www.pcn.minambiente.it/

Simeoni, L., Ferro, E., 2015. Displacement rates of extremely slow landslides. In: XVI ECSMGE, Edinburgh (UK), 13-17 September 2015, 1879-1884.

Simeoni, L., Puzzilli, L.M. 2017. Sliding surfaces and displacement rates of extremely-slow landslides: reliability of inclinometer measurements. In: 19th ICSMGE, Seoul, 17-22 September 2017, 3281-3284.

Simeoni, L., Ronchetti, F., Corsini, A., Mongiovì, L., 2015. Partial reactivation of a DGSD of ignimbrite and tuff in an alpine glacial valley in Northern Italy. Proc. of the Workshop on Volcanic Rocks and Soils, Isle of Ischia, Italy, 24-25 September 2015, 431-438. ISBN 978-1-138-02886-9.

Soldati M. (2013) Deep-seated Gravitational Slope Deformation. In: Bobrowsky P.T. (eds) Encyclopedia of Natural Hazards. Encyclopedia of Earth Sciences Series. Springer, Dordrecht.

Strozzi T., Farina P., Corsini A., Ambrosi C., Thüring M., Zilger J., Wiesmann A., Wegmüller U., Werner C., 2005. Survey and monitoring of landslide displacements by means of L-band satellite SAR interferometry. Landslides (Springer) 2 (3), 193 – 201.

Tombolato, S., Pedrotti, M., Simeoni, L. & Mongiovì, L. 2011. Field monitoring of a motorway viaduct moving on an extremely slow landslide; Proc. of the 8th International Symposium on Field Measurements in Geomechanics. Berlin, 12-16 Sept 2011, J. Gattermann and B. Bruns (Eds), ISBN: 3-927610-87-9.

Wasowski J., Bovenga F., 2014. Investigating landslides and unstable slopes with satellite Multi Temporal Interferometry: Current issues and future perspectives. Engineering Geology 174, pp. 103–138. http://dx.doi.org/10.1016/j.enggeo.2014.03.003.

Wasowski J., Pisano L., 2019. Long-term InSAR, borehole inclinometer, and rainfall records provide insight into the mechanism and activity patterns of an extremely slow urbanized landslide. Landslides. DOI 10.1007/s10346-019-01276-7

Author Contribution Statement

https://www.elsevier.com/authors/journal-authors/policies-and-ethics/credit-author-statement

The Authors spent similar efforts both to carry out the research and to write the paper. Lucia Simeoni's work dealt mainly with the geotechnical study, Francesco Ronchetti and Alessandro Corsini mainly contributed to the geological study.

Declaration of interests

☒ The authors declare that they have no known competing financial interests or personal relationships that could have appeared to influence the work reported in this paper.

☐The authors declare the following financial interests/personal relationships which may be considered as potential competing interests:

Highlights

- Study of large, composite and extremely slow landslides requires extensive multi-method monitoring of displacements

- Systematic errors affecting the measurements may mask the actual rate of movement

- Redundancy and coherence tests of monitoring data as a tool to check reliability of data and results

- The reliability of displacement monitoring is crucial to analyse large extremely slow landslides